

A boundary integral equation method in short-wavelength-to-period diffraction on multilayer 1D gratings and rough mirrors

Leonid I. Goray

St. Petersburg Physics and Technology Center for Research and Education, Russian Academy of Sciences, Russia and Institute for Analytical Instrumentation, RAS, Russia; e-mail: lig@pcgrate.com

Diffraction problems by 1D multilayer structures having arbitrary border profiles including edges are considered at smallest wavelength-to-period ratios. The integral equation theory is so flexible that one can point out a few areas of its modifiability. In this work special attention is paid to physical models and low-level details, as well as to the generalization of the power balance criterion for the case of absorbing gratings. In the case of shallow gratings and mirrors, introducing speed-up terms produces an adverse numerical effect because of the ensuing uncontrolled growth of coefficients in analytically improved asymptotic estimations.

1 INTRODUCTION

It is well-known that solution of the 2D Helmholtz equation with any rigorous numerical code meets with difficulties at small wavelength-to-period ratios ($\lambda/d \ll 1$) [1]. While the Standard Boundary Integral Equation methods (*SIMs*) are robust, reliable, and efficient, they exhibit poor convergence and loss of accuracy in the high-frequency range due to numerical contamination in quadratures. Increasing matrix size and enhancing computation precision, as well as application of convergence speed-up techniques, which are successfully explored in low- and mid-frequency ranges, lead to unreasonably stringent requirements for computing times and storage capacities in high and, especially, ultrahigh frequency ranges ($\lambda/d < 1.E - 2$ and $\lambda/d < 1.E - 3$).

This work is a part of the research that has been pursued over a long period of time with the purpose of developing accurate and fast numerical algorithms, including commercial ones designed to work at all, including the shortest, wavelength ranges [2, 3]. We consider diffraction from 1D multilayer structures with arbitrary border profiles, including edges and random roughnesses. The term "1D" refers to a general 1D grating or rough mirror on a planar surface which is periodic in one surface direction, constant in the second, and has a finite

number of borders and layers in the third one. The actual number of identical or different borders and layers can be large enough—up to a few thousands for x-ray applications. Though various approximated analyses [4, 5] developed for treatment of such challenging diffraction problems enjoy more or less successful application, they are always plagued with uncertainties which make comparison between rigorous and non-rigorous approaches difficult.

The boundary integral equation theory is so flexible that we can point out a few areas of its modifiability [6]. They are: (1) Physical model (choice of boundary types and conditions); (2) Mathematical structure (integral representations using potentials and a multilayer scheme); (3) Method of discretization (choice of trial functions, discretization scheme and treatment of corners in boundary profile curves); (4) Low-level details (calculations and optimization of Green's functions and their derivatives, mesh of collocation points, quadrature rules, solution of linear systems, caching of repeating quantities, etc.). A self-consistent explanation of various integral methods is well beyond the scope of this paper, and one should rather be addressed to the references. In this work, special attention is paid to (1) and (4) of the described Modified Boundary Integral Equation method (*MIM*) for small λ/d ratios, as well as to a generalization of power balance criteria for the case of absorbing gratings.

2 PRINCIPAL DIFFERENCE IN CONVERGENCE BETWEEN *SIM* AND *MIM* AT $\lambda/d \ll 1$

Convergence of the *SIM* and *MIM* is demonstrated for a simple case of diffraction on a plane transmission border (normal incidence in vacuum with the lower-medium refractive index $n_1 = 1.5$). For $\lambda/d = 1$ in Fig. 1, the convergence rate reached with speed-up techniques is high, with the Energy balance error of $\sim 1.E - 6$ in both polar-

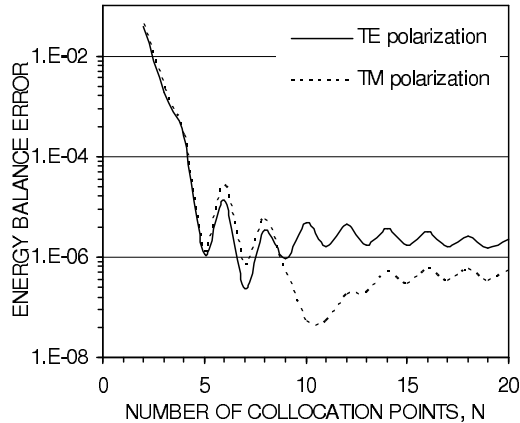


Figure 1: Using the *SIM* for the problem of diffraction on a plane interface for $\lambda/d = 1$ (normal incidence, $n_0 = 1$, $n_1 = 1.5$).

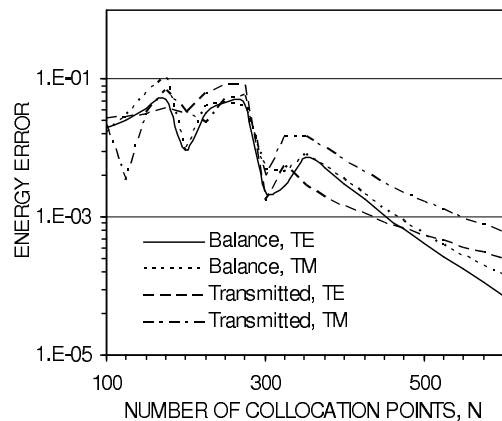


Figure 2: Same as Fig. 1 but for $\lambda/d = 0.01$.

ization states for the number of collocation points $N = 10$. For $\lambda/d = 0.01$ in Fig. 2, the convergence rate, again obtained with speed-up techniques, is low with the Energy balance and Transmitted energy errors of $\sim 1.E - 3$ in both polarizations for $N = 500$. The difference between the TE and TM transmitted energies for $N < 300$ is seen to be large, $\sim 1.E - 1$. For $\lambda/d = 1.E - 3$ in Fig. 3, the convergence rate calculated with speed-up techniques is very low, with the Energy balance error of $\sim 1.E - 2$ in both polarizations for $N = 1000$. As seen from Fig. 3, convergence of the series deteriorates for $N > 1000$ as the distance between the Green function's arguments tends to 0 (we use the Nyström collocation method [7]).

In contrast to the data of Figs. 2–3, the results

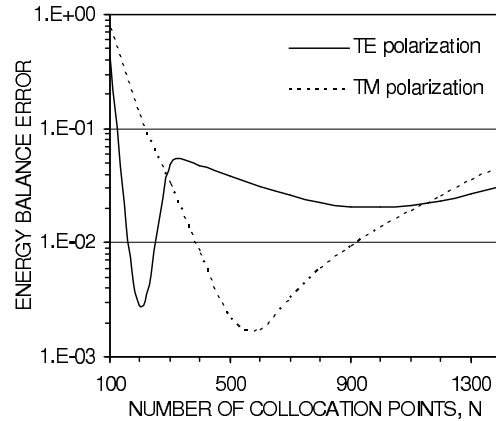


Figure 3: Same as Fig. 1 but for $\lambda/d = 0.001$.

for $\lambda/d = 1.E - 6$ obtained without application of any speed-up techniques exhibit the fastest convergence rate with a negligible Energy balance error (on the order of the computer accuracy) for $N = 2$ only. The most important among the convergence speed-up options which have to be switched off in this case is the allowance for logarithmic singularity, and second important, is the correction employed to account for the cut-off terms in the expansions of Green's functions and their normal derivatives (Aitken's term δ^2 in our case [6]). Such calculations depend also significantly on the summation rule chosen for the Green's series (see Sec. 3). While the results presented in Figs. 1–3 may certainly be different for various realizations of the method and of the speed-up techniques used, the overall pattern remains the same.

3 A SUMMATION RULE FOR GREEN'S SERIES

The *SIM* and *MIM* specify the number of positive and negative members in Green's function and their normal derivative expansions [6]. In the simplest case typical of real problems, the series are truncated symmetrically at the lower summation index $-P$ and the upper index $+P$, where P is an integer defined by $P \approx gN$. The truncation ratio g is optimized for small values of N and is kept constant as N increases. It was found that $g = 1/2$ is a reasonably good choice for most practical computations and, in particular, for small λ/d ratios.

Typical dependences on g for the above example with $\lambda/d = 1.E - 2$ are shown in Fig. 4. The Energy balance is closer to 1 and TE/TM Transmitted energies are close to each other at $g \approx 0.5$, with di-

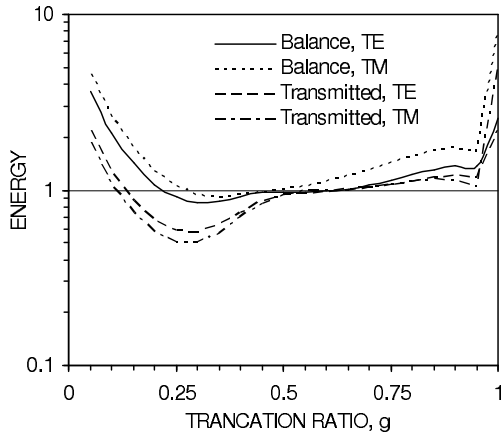


Figure 4: Using the *SIM* for the same problem as in Fig. 2 for $N = 100$.

vergence seen to set in at smaller and larger values of g . While today this rule is no more than empirical, there can be no doubt whatsoever that this choice is valid, and this has been verified in many realistic examples during the recent years. Note that in the *SIM* developed in [8], $g = 2/3$ for the resonance domain and should be varied for different λ/d ratios. It is worth noting that $g = 2/3$ is worse than $g = 1/2$ because the computation time is proportional to $2PN^2$.

A few words regarding the extent to which calculations made in extremely hard cases can be trusted are in order here. The workability of the programs has been confirmed by numerous tests usually employed in non-extreme cases: the reciprocity theorem, stabilization of results under doubling of N and variation of g , comparison with analytically amenable cases of plane interfaces, consideration of the inverse (non-physical) radiation condition, insertion of fictitious boundaries, variation of collocation point distribution, comparison with the results obtained by another of our codes or with published data, or with data corresponded to us by other researchers. The most important accuracy criteria based on a single computation is the Energy balance that can be generalized to include the lossy case.

4 GENERALIZATION OF THE ENERGY BALANCE CRITERIA FOR LOSSY GRATINGS

If the grating is perfectly conducting, then the conservation of energy is expressed by the standard

energy criterion

$$R = 1, \quad (1)$$

where R is the sum of the reflection order efficiencies.

If the grating is lossless, $\text{Im } n_l = 0, l = 0, \dots, M, M + 1$ is the number of layers; then conservation of energy is expressed by a similar energy criterion

$$R + T = 1, \quad (2)$$

where T is the sum of the transmission order efficiencies.

In a general case,

$$A + R + T = 1, \quad (3)$$

where A is called *the absorption coefficient* or simply the Absorption in the given diffraction problem. Besides being physically meaningful, the sum in (3) is very useful as one of numerical accuracy tests for computational codes and especially important in the x-ray and extreme ultra-violet (EUV) ranges, where absorption plays a predominant role. In the lossy case, one needs an independently calculated quantity A to verify Eq. (3). For such a quantity, we use the absorption integral defined in [7] and derived below.

Because of the problem being invariant under translation by an integer number of periods along the axis perpendicular to the grooves, one may restrict oneself to an analysis of the heat power loss \tilde{E}_A per grating period. \tilde{E}_A can be calculated as a difference between the energy fluxes that have crossed the upper, Γ_1 , and the lower, Γ_M , boundaries of the multilayer structure through an element of area bounded by the $x = 0, x = d$ and $z = 0, z = 1$ planes:

$$\tilde{E}_A = \int_0^1 dz \int_{\Gamma_1} \mathbf{S}_1^- \mathbf{n}_1 dl - \int_0^1 dz \int_{\Gamma_M} \mathbf{S}_M^- \mathbf{n}_M dl, \quad (4)$$

where \mathbf{S}_1^- and \mathbf{S}_M^- are time-averaged complex Poynting vectors calculated at the upper and lower boundaries on the floor, \mathbf{n}_1 and \mathbf{n}_M are unit vectors of the normal with components n_{1x}, n_{Mx} and n_{1y}, n_{My} , which are interior to the regions under study, and integration is performed along the cut of the boundaries by the $z = 0$ plane. Recalling that $|\mathbf{S}_j^-| = 0.5 \text{Re } \mathbf{E}_j^- \times \mathbf{H}_j^{-*}$, where \mathbf{E}_j^- and \mathbf{H}_j^- are complex vectors of the electric and magnetic fields calculated on the floor at the $j = 1, M$ boundary, and X^* denotes complex conjugate of X , we open

the vector and dot products for the TE and TM polarizations under the integral signs in Eq. (4):

$$\begin{aligned}\tilde{E}_A(TE) &= 0.5\text{Re}\left[\int_{\Gamma_1} E_z^-(H_x^{-*}\cos\beta - H_y^{-*}\cos\alpha)dl\right. \\ &\quad \left.- \int_{\Gamma_M} E_z^-(H_x^{-*}\cos\beta - H_y^{-*}\cos\alpha)dl\right], \\ \tilde{E}_A(TM) &= 0.5\text{Re}\left[\int_{\Gamma_1} H_z^{-*}(E_x^- \cos\beta - E_y^- \cos\alpha)dl\right. \\ &\quad \left.- \int_{\Gamma_M} H_z^{-*}(E_x^- \cos\beta - E_y^- \cos\alpha)dl\right]. \quad (5)\end{aligned}$$

As follows from Maxwell's equations:

$$\begin{aligned}dE_z^{-*}/dn &= (-H_y^{-*}\cos\alpha + H_x^{-*}\cos\beta)/(i\omega\mu_l), \\ dH_z^-/dn &= (-E_y^- \cos\alpha + E_x^- \cos\beta)/(i\omega\epsilon_l), \quad (6)\end{aligned}$$

where ϵ_l and μ_l are the electric permittivity and magnetic permeability of layer l , ω is the frequency of the electromagnetic field, and i is the imaginary unit. Substituting Eq. (6) in Eq. (5), we obtain:

$$\begin{aligned}\tilde{E}_A(TE) &= 0.5\text{Re}\left[\int_{\Gamma_1} \frac{1}{i\omega\mu_1} \frac{dE_z^{-*}}{dn} E_z^- dl\right. \\ &\quad \left.- \int_{\Gamma_M} \frac{1}{i\omega\mu_M} \frac{dE_z^{-*}}{dn} E_z^- dl\right], \\ \tilde{E}_A(TM) &= 0.5\text{Re}\left[\int_{\Gamma_1} \frac{1}{i\omega\epsilon_1} \frac{dH_z^-}{dn} H_z^{-*} dl\right. \\ &\quad \left.- \int_{\Gamma_M} \frac{1}{i\omega\epsilon_M} \frac{dH_z^-}{dn} H_z^{-*} dl\right]. \quad (7)\end{aligned}$$

In studies of electromagnetic field losses at the grating, \tilde{E}_A , it should be normalized against the heat power losses of the incident wave \tilde{E}_A^i within a plane element of area bounded by the same planes $x = 0, x = d$ and $z = 0, z = 1$ and having an optical constant $\sqrt{\epsilon_1\mu_1}$ equal to that of medium 1. By canceling the same factor $\exp(-i\alpha_0^i x)$ in the expressions for the incident and diffracted fields in a diffraction problem [9] and taking account of the plane surface of derivation, the explicit forms of the incident field of unit amplitude and of its normal derivative can be simplified to $\exp(-i\beta_0^i y)$ and $\exp(-i\beta_0^i y)(-i\beta_0^i)$, respectively, where α_0^i and β_0^i are x and y components of the incident wave vector. Substituting this in Eq. (7) and recalling the

boundary conditions we come to

$$\tilde{E}_A^i(TE) = 0.5\frac{\beta_0^i d}{\omega\mu_0}, \tilde{E}_A^i(TM) = 0.5\frac{\beta_0^i d}{\omega\epsilon_0}. \quad (8)$$

Using (7) in conjunction with (8), the normalized expressions for energy absorbed in the grating are given by:

$$\begin{aligned}A(TE) &= \frac{\tilde{E}_A(TE)}{\tilde{E}_A^i(TE)} = \frac{1}{\beta_0^i d} \text{Re}\left[\int_{\Gamma_1} \frac{i\mu_0}{\mu_1} \frac{dE_z^{-*}}{dn} E_z^- dl\right. \\ &\quad \left.- \int_{\Gamma_M} \frac{i\mu_0}{\mu_M} \frac{dE_z^{-*}}{dn} E_z^- dl\right], \\ A(TM) &= \frac{\tilde{E}_A(TM)}{\tilde{E}_A^i(TM)} = \frac{1}{\beta_0^i d} \text{Re}\left[\int_{\Gamma_1} \frac{i\epsilon_0}{\epsilon_1} \frac{dH_z^-}{dn} H_z^{-*} dl\right. \\ &\quad \left.- \int_{\Gamma_M} \frac{i\epsilon_0}{\epsilon_M} \frac{dH_z^-}{dn} H_z^{-*} dl\right]. \quad (9)\end{aligned}$$

Recalling that $\text{Re } X = \text{Im } iX$, Eq. (9) for the universal field components u_j^\pm and their normal derivatives v_j^\pm (u_j^+ and v_j^+ calculated at the boundary on the ceiling) can be recast to the form

$$A = \frac{1}{\beta_0^i d} \text{Im}\left[\int_{\Gamma_1} u_1^+ v_1^{+*} dl - c \int_{\Gamma_M} u_M^- v_M^{-*} dl\right], \quad (10)$$

where $c = \mu_0/\mu_M$ is for the TE, and $c = \epsilon_0/\epsilon_M$, for the TM polarization. Eq. (10) for the absorption of an electromagnetic field by a multilayer grating coincides with the expression reported in [7] and derived by applying the Green's formula to boundary functions for the contours in the upper and lower media. By definition, the first integral in Eq. (10) is $1 - R$, and the second, T , and it vanishes if the lower medium is absorbing [9] or the lower boundary is perfectly conducting. The sum $A + R + T$ is actually the energy balance for an absorbing grating, and the extent to which it approaches unity is a measure of the accuracy of a calculation.

5 EXAMPLES OF DIFFRACTION PROBLEM CALCULATIONS FOR $\lambda/d \ll 1$

Three types of small λ/d ratio problems are known from optical applications: (a) shallow gratings working in the x-ray and EUV ranges, both at near-normal and grazing incidence angles, (b) deep echelle gratings with a steep working facet illuminated along its normal by light of any wavelength,

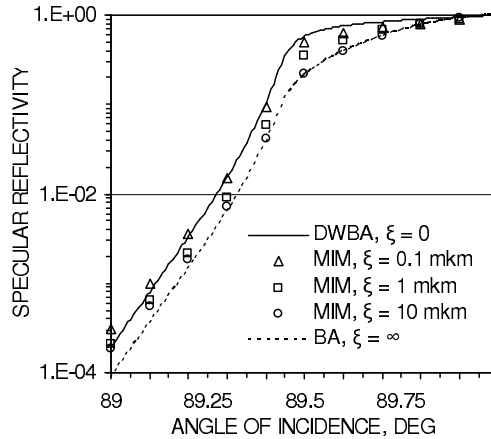


Figure 5: Specular TE reflectance of Au mirrors calculated for $\sigma = 1.5$ nm and different ζ for $\lambda = 0.154$ nm vs. angle of incidence.

and (c) rough mirrors and gratings in which rough borders can be represented by a grating with a large period d , and which contain a few or a large number of random asperities illuminated at any possible angle and wavelength [10]. To study the scattering intensity with the use of a forward electromagnetic code, one should first of all generate statistical realizations of the border profiles of the structure under investigation, then calculate the scattering intensity for each realization and, finally, average the intensities over all the realizations. To allow randomization of grating borders with a Gaussian height distribution and a Gaussian correlation function, the known spectral method was extended to include the case of non-plane interfaces prescribed by arbitrary polygons [10]. Non-plane borders are characteristic also of self-assembled low-dimensional quantum structures defined by other asperity statistics. For an investigation of specular and diffuse x-ray scattering from multiple ensembles of quantum dots in the *MIM* frame, the Reader is referred to Ref. [10].

An example of cases (a) and (c) combined can be found in [2, 10]; it is essentially a 20-pair Mo/Si-coated 4200 groove/mm EUV flight grating of the Sun mission Hinode. The physical model with a stack of plane interfaces over one non-planar interface can be used to advantage, due to its good accuracy and very high speed, for case (a) [3]. As to case (b), for echelles in which resonance on the working facet plays a predominant role, it is often, but not always, possible to 'rotate' the layer stack and consider a diffraction problem with the plane stack

parallel to the working facet rather than to the substrate. There are no mathematical approximations in this model except the numerical implementation. This approach generally works [3] in the case of thin layers (layer thickness-to-wavelength < 0.1), an area hard to cope with for *SIMs*. However, the sophisticated approach developed for single-coated echelles in [1] is fast with a high rate of convergence.

A gold x-ray mirror for use at grazing incidence near the angle of total external reflection was chosen as an example of case (c). The difference between the asymptotic and rigorous approaches can be clearly seen in Fig. 5 which plots the calculated specular TE reflectivity of Au surfaces with rms roughness $\sigma = 1.5$ nm vs. angle of incidence for $\lambda = 0.154$ nm and for different values of the lateral correlation length ζ . The reflection coefficients calculated rigorously in the low-intensity domain for $\zeta = 10\mu\text{m}$ are approximately twice those obtained with the Debye-Waller factor [10] which is commonly used in this region and derived in the frame of the first-order Born approximation (BA) [5]. For $\zeta = 0.1\mu\text{m}$, the excess is already about fourfold. By contrast, close to the critical angle the rigorous data obtained for $\zeta = 0.1\mu\text{m}$ lie $\sim 20\%$ below the values calculated for this region with the Nevot-Croce factor [10], which is derived in the frame of the first-order distorted-wave BA (DWBA) [5]. For $\zeta = 10\mu\text{m}$, in the region of high intensities, the differences are still larger, to reach finally a few hundred %. The behavior of reflectivity with ζ illustrated in Fig. 5 matches qualitatively with the results obtained in the frame of the second-order DWBA [11] while differing in quantitative estimates, particularly for values of ζ for which second-order DWBA does not work. To take into account the fine structure of the roughness in the above example, one has to use ~ 100 asperities per d , average over 9–25 random boundaries and assume $N = 400 \div 3200$. For $\zeta = 10\mu\text{m}$ and $d = 1500\mu\text{m}$, $\lambda/d \approx 1.E-7$, a value too small to be dealt with in any rigorous numerical approach. For *MIM*, however, this formidable scattering problem is found to be convergent and yields quite accurate results (Energy balance error $\sim 1.E-5$) for only $N = 400$ and no speed-up techniques invoked. The time taken up by one computation on a workstation with two Quad-Core Intel® Xeon® 2.66 GHz processors, 8 MB L2 Cache, Bus Clock 1333 MHz and 16 GB RAM, is about one minute when operating on Windows Vista® Ultimate 64-bit and employing eightfold paralleling.

6 CONCLUSION

The MIM works reliably and fast for very low λ or λ/d in the x-ray–EUV range, despite the small number of collocation points per wavelength used in the approach (it is also true for echelles). For example, if a period includes 50 collocation points and $\lambda/d = 1.E - 3$, there is only $5.E - 2$ point per wavelength. In this case, however, the profile depth, the bi-layer thickness, and the incident radiation wavelength must be of the same order of magnitude. The same rule for reaching the maximum diffraction efficiency is, on the whole, valid for longer wavelengths too.

The accurate results obtained by the rigorous method for the intensity of scattering from gratings and rough mirrors may differ substantially from those derived using known asymptotics and approximate approaches. These differences may give rise, for instance, to wrong estimates of rms roughness and correlation length if the latter are determined by comparing experimental data with calculations. Besides, the rigorous approach permits taking into account any known roughness statistics.

In the cases of shallow gratings and mirrors working at very small λ/d ratios, introducing speed-up terms produces an adverse numerical effect because of the ensuing uncontrolled growth of coefficients in analytically improved asymptotic estimations. With all speed-up options turned off, it is often possible to obtain for the most difficult problems surprisingly good convergence at orders of practical interest, and an energy balance very close to 1. However, treatment of such situations remains mostly a kind of art.

ACKNOWLEDGEMENTS

The author feels indebted to Sergey Sadov (Memorial NF University, Canada) for the information provided and fruitful collaboration. Helpful discussions and testing with Bernd Kleemann (Carl Zeiss, Germany) and Andreas Rathsfeld (WIAS, Germany) are greatly appreciated.

This work was partially supported by the Russian Foundation for Basic Research (grant N 06-02-17331).

REFERENCES

- [1] Rathsfeld A., Schmidt G. & Kleemann B. H., 2006, On a Fast Integral Equation Method for Diffraction Gratings, *Commun. Comput. Phys.*, **Vol. 1,6**, pp. 984–1009.
- [2] Goray L.I., Seely J.F. & Sadov S.Yu., 2006, Spectral separation of the efficiencies of the inside and outside orders of soft-x-ray–extreme-ultraviolet gratings at near normal incidence, *J. Appl. Phys.*, **Vol. 100,9**, pp. 094901-1–13.
- [3] Goray L.I., 2005, Numerical analysis of the efficiency of multilayer-coated gratings using integral method, *Nuclear Inst. Methods in Physics Research A*, **Vol. 536,1–2**, pp. 211–221.
- [4] Babich V.M. & Buldyrev V.S., 2007, Asymptotic Methods in Short-Wavelength Diffraction Theory, Alpha Science Series on Wave Phenomena, 480 p.
- [5] Elfouhaily T.M. & Guerin C.-A., 2004, A critical survey of approximate scattering wave theories from random rough surfaces, *Waves Random Media*, **Vol. 14**, pp. R1–R40.
- [6] Goray L.I. & Sadov S.Yu., 2006, Numerical modeling of coated gratings in sensitive cases, *Diffraction Optics and Micro-Optics*, OSA TOPS **Vol. 75**, pp. 365–379.
- [7] Goray L.I., Kuznetsov I.G., Sadov S.Yu. & Content D.A., 2006, Multilayer resonant sub-wavelength gratings: effects of waveguide modes and real groove profiles, *J. Opt. Soc. Am. A*, **Vol. 23,1**, pp. 155–165.
- [8] Maystre D., 1980, Electromagnetic Theory of Gratings, *Topics in Current Physics*, **22**, p. 98.
- [9] Goray L.I. & Seely J.F., 2002, Efficiencies of master replica, and multilayer gratings for the soft-x-ray–extreme-ultraviolet range: modeling based on the modified integral method and comparisons with measurements, *Appl. Opt.*, **Vol. 41,7**, pp. 1434–1445.
- [10] Goray L.I., 2007, A rigorous solution for electromagnetic scattering from any kind of asperities of multilayer 1-D structures in the X-ray–VUV ranges, *Proc. SPIE*, **Vol. 6617**, pp. 661719-1–12.
- [11] De Boer D.K.G., 1994, Influence of the roughness profile on the specular reflectivity of x rays and neutrons, *Phys. Rev. B*, **Vol. 49,9**, pp. 5817–5820.